ELEMENTA
Science of the Anthropocene

Estimating Arctic sea-ice freeze-up and break-up from the satellite record: A comparison of different approaches in the Chukchi and Beaufort Seas

Mark Johnson[1*] • Hajo Eicken[2]

[1]School of Fisheries and Ocean Sciences & College of Natural Sciences and Mathematics, University of Alaska Fairbanks, Alaska, United States
[2]International Arctic Research Center, University of Alaska Fairbanks, Alaska, United States
*majohnson@alaska.edu

Domain Editor-in-Chief
Jody W. Deming, University of Washington

Associate Editor
Stephen F. Ackley, University of Texas at San Antonio

Knowledge Domain
Ocean Science

Article Type
Research Article

Received: February 15, 2016
Accepted: July 14, 2016
Published: September 1, 2016

1. Abstract

The recognized importance of the annual cycle of sea ice in the Arctic to heat budgets, human behavior, and ecosystem functions, requires consistent definitions of such key events in the ice cycle as break-up and freeze-up. An internally consistent and reproducible approach to characterize the timing of these events in the annual sea-ice cycle is described. An algorithm was developed to calculate the start and end dates of freeze-up and break-up and applied to time series of satellite-derived sea-ice concentration from 1979 to 2013. Our approach builds from discussions with sea-ice experts having experience observing and working on the sea ice in the Bering, Chukchi and Beaufort Seas. Applying the algorithm to the 1979–2013 satellite data reveals that freeze-up is delayed by two weeks per decade for the Chukchi coast and one week per decade for the Beaufort coast. For both regions, break-up start is arriving earlier by 5–7 days per decade and break-up end is arriving earlier by 10–12 days per decade. In the Chukchi Sea, "early" break-up is arriving earlier by one month over the 34-year period and alternates with a "late" break-up. The calculated freeze-up and break-up dates provide information helpful to understanding the dynamics of the annual sea-ice cycle and identifying the drivers that modify this cycle. The algorithm presented here, and potential refinements, can help guide future work on changes in the seasonal cycle of sea ice. The sea-ice phenology of freeze-up and break-up that results from our approach is consistent with observations of sea-ice use. It may be applied to advancing our understanding and prediction of the timing of seasonal navigation, availability of ice as a biological habitat, and assessment of numerical models.

2. Introduction

The annual cycle of Arctic sea ice, from freeze-up to break-up, currently contracts and expands across an area ranging from 7 to 16 x 10^6 km^2 (Serreze et al., 2007). Sea-ice extent affects the fluxes of sensible and latent heat and modifies the regional surface albedo. Based on satellite data from 1979 to 2000, the perennial Arctic sea-ice cover is declining at –7% per decade. Including the years through 2013, the Arctic-wide trend is –14% per decade (Stroeve et al., 2014a,b).

Trends in satellite-derived surface brightness temperature suggest a lengthening of the melt season (Comiso, 2002; Parkinson, 2014). Melt onset is particularly affected by early season atmospheric storms that bring warm air at the same time that incident solar energy increases in May (Bitz et al., 1996; Perovich and Polashenski, 2012). Late spring atmospheric forcing, at the onset of melt, influences low-frequency variability sometimes for decades through nonlinearities in sea-ice volume (thickness and extent), based on energy balance models forced by anomalous melt onset dates (Bitz et al., 1996). Using an energy balance model, Bitz and Roe (2004) found that variations in season length had a "nontrivial" influence on sea-ice thickness even though the sea-ice growth-thickness relationship, where thin ice grows faster thermodynamically than thick ice, dominates the overall ice behavior.

It is well known that melt season heat loss is enhanced in regions of thin ice and open water that permit large fluxes of sensible heat, moisture and long-wave radiation to the atmosphere. For example, the net heat loss from limited areas of open water exceeds heat loss from the ice pack (Smith et al., 1990). With two-thirds of the heat absorbed by the ocean from June through July (Perovich and Polashenski, 2012), changes in the timing of ice freeze and melt rather than total incident energy dominate regional oceanic heat budgets (Perovich et al., 2007, 2011; Stroeve et al., 2014b). Because the incident solar energy is large at the time of melt onset, the total solar energy absorbed by the ice and ocean depends on the timing of melt onset more so than the melt season duration. Earlier melt allows 8.7 MJ m^{-2} of solar energy per day to be absorbed while freeze-up delays allow 1.5 MJ m^{-2} per day to be absorbed (Perovich et al., 2007).

Beyond their relevance to the heat budget of Arctic seas, the geographical patterns and timing of freeze-up and break-up influence human behavior and ecosystem functions in the Arctic. Coastal communities depend on the presence of shorefast ice for a range of activities including subsistence hunting and travel among villages (Eicken et al., 2009; Laidler et al., 2009). The oil and gas industry uses landfast sea ice as a platform for wintertime operations. Drifting ice constitutes a major hazard to offshore operations and maritime traffic (Eicken et al., 2009; Stephenson et al., 2011; Eicken and Mahoney, 2015). A number of protected marine species, including polar bears, walrus and ice seals, rely on ice cover as a platform during critical periods in the animals' life cycle (Post et al., 2013). Hence, shifts in basin-scale patterns of freeze-up and break-up, as indicated by recent studies based on remote-sensing (e.g., Stroeve et al., 2014b; Parkinson, 2014), have major impacts on people and ecosystems because of both reductions in the length of the ice season and increased rates of seasonal ice retreat.

Management of marine living resources and human activities requires clear and consistent definitions of key dates and events in the annual ice cycle since these in turn are critical elements of regulatory or informal rule sets (Lovecraft et al., 2013). Freeze-up and break-up are of disproportionately high importance because they define the summer operational window for coastal communities and industry. Freeze-up and break-up are important periods in marine mammal life cycles such as rearing of seal pups or the seasonal whale migration. Consistency and interoperability are also critical for operational forecasts of ice conditions and tracking of potential hazards during the spring and fall transition seasons (Eicken, 2013). At present, however, we are lacking consistent definitions of such key events in the ice cycle as freeze-up and break-up. This is a problem of some urgency considering recent increases in shipping and offshore resource exploration in the Arctic that rely on and require unambiguous regulatory frameworks.

We recognize that many individual studies of changes in the Arctic sea-ice season have employed internally consistent definitions of freeze-up, but among different studies these definitions vary widely. In some of the earliest work based on remote-sensing data, dates of snowmelt onset (with melt onset and break-up typically used interchangeably) were determined from Scanning Multichannel Microwave Radiometer (SMMR) data from 1979 through 1998 using melt signatures from 18- and 37-GHz brightness temperature changes that showed zones of early melt onset near the Siberian coast and late melt near Baffin Bay (Drobot and Anderson, 2001). Based on data from April through July for 1979 and 1980, Anderson (1987) showed an Arctic melt pattern that began in the Chukchi Sea and progressed westward, and a pattern that began in the Kara and Barents Seas and expanded to the Laptev Sea region. In the Chukchi Sea region, Anderson (1987) found the date of initial melt from the 1979 and 1980 SSMR data to vary generally by 7 to 10 days with a maximum of 25 days.

Parkinson (2014) showed trends in changes of the pan-Arctic sea-ice season length where the length of the sea-ice season was defined by counting the total number of days in each year having ice concentration exceeding 15% for each grid point of ice concentration from the passive microwave satellite remote-sensing data. Trends in the number of days per year of ice concentration above 15% were calculated for periods of 10, 20, 30 and 35 years. The record length (1979–2013) trends for Arctic areas at or above 10^6 km^2 ranged from –30 to +10 days per decade (see Parkinson's Figure 2).

Markus et al. (2009) and Stroeve et al. (2014b) examined changes in the length of the Arctic melt season using passive microwave brightness temperatures that are sensitive to the liquid water content in snow pack. Melt onset and freeze onset were defined as the first day when melting or freezing became continuous. They defined early melt onset as the first day melt is detected, and defined early freeze onset as the first day freezing is detected. Markus et al. (2009) tracked the dates for early melt onset and continuous melt (EMO, MO) and early and continuous freeze onset (EFO, FO) to establish endpoint dates for "inner" (MO to EFO) and "outer" (EMO to FO) melt seasons. Using these definitions, they computed averages and trends for ten Arctic regions (see their Figure 8) using data from 1979 to 2007. Note that Markus et al. (2009) use "freezeup" interchangeably with freeze onset, a use distinctly different from freeze-up as defined in this paper and described below.

Mortin et al. (2014) derived melt-freeze transition dates from active microwave remote-sensing data for 1999–2012 by extending the QuickSCAT record using ASCAT data. A comparison with data by Markus et al. (2009) showed generally good agreement, but with substantial deviations by up to one month in freeze and melt onset for some regions. The derived melt-freeze transitions from QuickSCAT (13.4GHz) from 1999 to 2009, and from ASCAT (5.3GHz) from 2006, provided information on the pan-Arctic melt-freeze

transitions from 1999 through 2012 poleward of 60°N at 4.5 km resolution. Similar to passive-microwave approaches, scatterometer data respond to changes in surface snow and ice dielectric properties which may or may not relate to geophysically or operationally relevant parameters. To eliminate unreasonable melt-freeze transitions, Mortin et al. (2014) relied on sea-ice concentration data from the Special Sensor Microwave/Imager (SSM/I) and Special Sensor Microwave Imager/Sounder (SSMI/S) instruments. Using SSM/I and SSMI/S to constrain estimates of melt-freeze transitions suggests those data have additional utility in studies of the annual cycle of sea ice.

An analysis of abrupt sea-ice changes using ensemble numerical simulations by Holland et al. (2006) found that the dynamic effects of ice transport and ridging had "little direct role" in climate transitions and instead were thermodynamically driven. However, thermodynamic melt onset does not necessarily correspond to the first appearance of open ocean, although changes in microwave emissivity are sometimes erroneously taken for a break-up signal which is a process combining dynamics with thermodynamics. The emissivity spectrum is difficult to relate to specific ice surface type (Baordo and Geer, 2015). While some of the aforementioned studies validated or calibrated their approach based on surface air temperature or satellite-derived ice concentration data, we are not aware of research that compares or validates remote-sensing derived data against ground-based observations of freeze-up or break-up.

In this study, we are motivated by three issues relevant to determining the timing of the annual sea-ice cycle.

(1) The character of sea ice is changing, including declining ice (Bjørgo et al., 1997; Parkinson et al., 1999) and thinning ice (Rothrock et al.,1999; Wadhams and Davis, 2000). The seasonal ice cycle is changing based on thermodynamic phase changes (Markus et al., 2009), and the length of the open water season is changing based on the 15% ice concentration threshold (Parkinson, 2014). In this paper we examine the timing and duration of the ice season by defining freeze-up and break-up having ecological significance, relating to human activities, and reflecting what users of the ice and ocean see. This approach draws on long-term observations by sea-ice experts in several Alaskan coastal communities (Eicken et al., 2014). Thus, when "freeze-up" occurs, persistent ice ends the "open water" season. When sea ice "breaks up" it permits seasonal travel on the ocean. Our work is particularly motivated by the need to arrive at an intercomparable, meaningful index of sea-ice phenology. Such phenology should be relevant to ice users, such as humans navigating and hunting on and among sea ice, useful to characterizing the ecological roles of the ice, and internally consistent to be meaningful to large-scale geophysical studies of sea ice.

(2) Analyzing passive-microwave derived ice concentrations for the Arctic from 1979 to 2013, we arrive at time series of freeze-up and break-up that allow us to examine and compare variability and trends. We rely on ice concentration from passive microwave measurements because that data set is well validated and well understood. Of particular interest is that the passive microwave data from 1979 onwards provide a longer context for changes in sea-ice phenology than recent studies (e.g., Brown et al., 2014) where the choice of sensors shifts the focus to the current decade.

(3) Using the passive microwave data from 1979 through 2013, we derive and analyze the timing of freeze-up and break-up in the coastal region of the Chukchi and Beaufort Seas in light of community-based observations of the ice cycle, sea-ice uses, and ice hazards. This region is of interest because it has experienced some of the largest changes in seasonal minimum ice extent (Parkinson, 2014) anywhere in the Arctic, with major increases in solar heating of the surface ice-ocean system (Perovich et al., 2011; Stroeve et al., 2014b) and implications for coastal dynamics (Barnhart et al., 2014). Comparing these data to other measures of freeze-up or break-up provides insight into potential biases and uncertainties of different approaches taken to determine key events in the ice cycle for operational or regulatory purposes.

Figure 1 illustrates the problem at hand by comparing five different measures of sea-ice seasonality and specifically freeze-up for the nearshore region off Barrow, Alaska. The methods address the last day of navigation, direct observations of freeze-up, presence of shore ice from Radarsat SAR, and the remote-sensing approach introduced here. There is a great deal of variation among the different methods. From 1990 to 2013, the dates shown in Figure 1 for "persistent ice", "freeze-up" and "last day of navigation" span more than two months, providing little clarity on the behavior of sea ice at that time, or from year to year. Depending on the specific use of the ice cover or the locally relevant definition, observations by local experts at the same site may not agree. Here we attempt to resolve the problem by developing a coherent framework for analyzing and characterizing the timing of freeze-up and break-up.

3. The sea-ice seasonal cycle of the coastal Chukchi and Beaufort Seas

Barry et al. (1979) used LANDSAT imagery from 1973 through 1977 to characterize the extension/modification of fast ice for the central Chukchi coast from November through February (see their Table 1). They observed that "first openings and movement" of the ice were on June 10 and "new ice begins to form in October" with the actual freeze-up date varying by 10–15 days. Barry et al. (1979) noted that the fast ice off Icy Cape and Peard Bay (Chukchi coast) has melt and breakup characteristics similar to that along the Beaufort Sea coast.

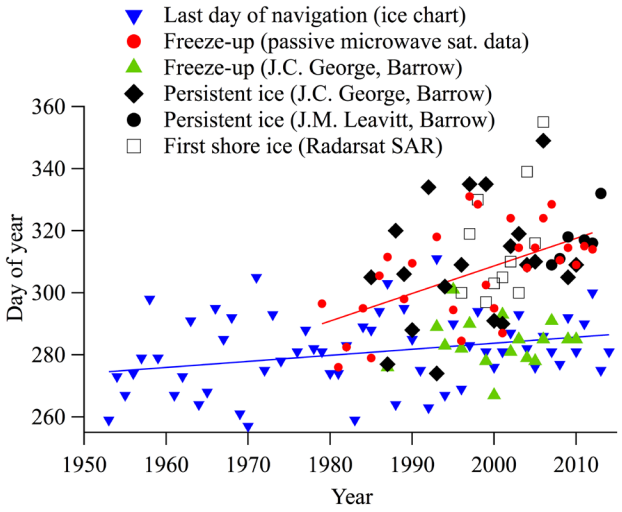

Figure 1
Methods of measuring freeze-up.

Last day of navigation from the Barnett Ice Severity Index (blue), freeze-up as calculated here (red), freeze-up based on direct observations at Barrow by local observer J.C. George (green), date of first persistent ice noted by local observers J.C. George and J.M. Leavitt (black), and first shore ice from Radarsat SAR (white squares). Blue and red lines are linear fits to the data.

doi: 10.12952/journal.elementa.000124.f001

Break-up along the Chukchi coast is driven by solar heating and atmospheric and oceanic dynamics (Barry et al., 1979; Petrich et al., 2012). The first open water is along the margin of the shorefast ice. The 20-m isobath, a proxy for grounded ridges stabilizing shorefast ice farthest away from the coast, is generally 10 to 25 km offshore in the Chukchi Sea and about twice that distance off the Beaufort Sea coast (Mahoney et al., 2014).

Ice conditions in the Beaufort Sea are different from conditions in the Chukchi Sea (Barry et al., 1979; Mahoney et al., 2014). The annual cycle for the Beaufort Sea begins with freeze-up over the low-salinity inner shelf and proceeds as follows (Barry et al., 1979; Mahoney et al., 2014) with approximate timing: 1) new ice formation near shore (October); 2) freezing in sheltered bays and lagoons; 3) seaward extension of the ice sheet in late fall and early winter (October–November) and disruption of the ice by late-winter storms (December–February) and pressure from the pack ice; 4) generally stable ice shoreward of the 15-m isobath in late winter and early spring (February–May); 5) over-ice flooding at the river mouths in spring (May); 6) surface melt and pond formation on the ice surface (May–June); 7) cracks or flaws in previously continuous ice sheets (June); 8) movement of previously immobile ice; and finally 9) nearshore regions becoming largely free of ice (July–August).

Along the Beaufort Sea coast, a stable and relatively smooth fast ice sheet is present between the coast and the barrier islands from January through May. Because the barrier islands extend along more than half of the 800 km coast, fast ice in the Beaufort Sea is well anchored and protected from pack ice seaward of the islands (Barry et al., 1979). The offshore region was characterized by Kovacs and Mellor (1974) and Reimnitz et al. (1978) as a zone of fast ice, grounded ridges, and seasonal ice pack.

Variations in break-up are due to the strength, thickness, and morphology of the ice and regional weather (Barry et al., 1979). Break-up in the Beaufort Sea, defined by "openings and movement", occurs after about 55–144 thawing degree days (TDDs, defined in °C) according to Barry et al. (1979). Clearing of the fast ice takes approximately 140–220 TDDs (°C). The first stage of break-up is flooding of the lagoons and estuaries in late May or early June (Barry et al., 1979) and at the mouths of the Colville, Sagavanirktok, and Kuparuk Rivers. (River deltas account for 16% of the total Beaufort Sea coast.) When rivers flood, nearby bottom fast ice floats up and cracks develop. Nearshore open water spreads laterally and seaward from mid-June through early July as melt ponds form and the ice sheet thins.

Table 1. Definitions of starting and ending dates of freeze-up and break-up

Starting or ending date	Criteria and algorithm
Start freeze-up	Date for which the sea-ice concentration exceeds the average value for August and September ("summer") plus one standard deviation for the first time. A minimum threshold is set to 15%.
End freeze-up	Date for which the sea-ice concentration exceeds for the first time the average ice concentration for January and February ("winter"), minus 10%.
Start break-up	Date for which the sea-ice concentration exceeds the threshold calculated as the last day for which the previous two weeks' ice concentration always exceeds the average value for winter (Jan-Feb), minus two standard deviations.
End break-up	Date for which the sea-ice concentration exceeds for the last time the average value for summer (Aug-Sep), plus one standard deviation. A minimum threshold is set to 15%.

doi: 10.12952/journal.elementa.000124.t001

Updating and extending the study of Barry et al. (1979), Mahoney et al. (2014) found that in recent years, landfast ice forms up to two weeks later and breaks up as much as two to four weeks earlier than in the mid-1970s based on Radarsat SAR data from 1996 through 2008. Note, however, that both datasets and definitions of freeze-up and break-up were not entirely consistent between the two studies, reinforcing the arguments made above for the need to develop a coherent analysis framework.

4. Methods: Approach for calculating freeze-up and break-up

Indigenous experts primarily in the coastal communities of Wales, Gambell and Barrow, Alaska, with collective knowledge of the Bering, Chukchi and Beaufort Seas have been keeping records of sea-ice, ocean, and weather conditions as part of the Seasonal Ice Zone Observing Network (SIZONet). This community-based observation component, described in detail by Eicken et al. (2014), has kept daily logs since 2006. Ice experts log weather, ocean and ice conditions relevant to activities and ice use by members of their respective communities. Log entries are transcribed and entered into a database for archival, sharing and analysis (Eicken et al., 2014). This work arrived at a representative seasonal ice cycle for 2006–2007 and then placed it in context of interannual variability from 2006 through 2011 of freeze-up and break-up dates.

Observations during the freeze-up season typically focused on ocean access for subsistence hunters, potential hazards due to the presence of slush ice, and the impact of freeze-up on animals and shoreline processes. Excerpts from two entries by Winton Weyapuk, Jr. from Wales during the 2007 freeze-up season illustrate the types of observations made (Apangalook et al., 2013):

> *Skies are mostly cloudy, winds NE at 30, gusting to 35 [mph], temp about 19 F, visibility 7 miles. Light drifting snow. There are narrow strips of light slush in the ocean. Small pieces of pancake ice washed ashore along the tide line. Frozen slush on the beach at the high tide line. Frost smoke not very visible. There are more extensive areas of light slush towards the North. A few clams are washing in. Large flocks of seagulls feeding along the breakers near the shore. […]. 7 Nov. 2007.*

> *Skies are partly cloudy, winds NE at 15 [mph], temp about 23 F, visibility 10 miles. There was occasional moderately heavy snow late in the morning. The slush berm created the day before has been knocked down to half its size or smaller. Thin slush in front of the village and to the North, thicker at the cove. The slush is still soft and not solid enough to walk on. Saw a few small seals just off the beach in front of the village. […] Winds are higher offshore with white caps visible about 4 to 5 miles out. Small areas of frost smoke out there where the waves are breaking. 9 Nov. 2007.*

Selected log entries by J. M. Leavitt during the time of freeze-up at Barrow provide insight into the freeze-up process, the criteria relevant to local observers in defining the nature of the ice present, and uncertainties associated with determining a freeze-up date.

1 November 2011: NW@16, 26°, Swell[s] are here at 5′. Slush ice goes about ½ mi out. Lots of seagulls along the beach, snowing 1.5 mi visibility[,] lots of slush ice has been build[ing] on the beach […]

11 November 2011: E@18, 5°, Open water as far as one can see, no ice in sight

12 November 2011: NE@27, –5°, Broken ice is near the beach blowing with the wind, another day of blowing snow, light flurries + cloudy

13 November 2011: N@15, 2°, Ice near the beach has stopped but moving about 200′ from the shore going to the SW, patches of open water here + there but mostly ice cover. All young ice from this fall, ice near the beach is still loose […]

15 November 2011: N@15, 11°, Ice near beach has froze over, minor buckling mostly all ice cover, few small ponds of water, all 1st year ice […]

17 November 2011: SW@10, 2°, All is [ice] as far as one can see, the small ponds also have froze over, ice near beach thick enough to walk on, ice is a[round] 200′ off the shore is whiter in color so it is a little thicker

As is evident from these observations, slush ice formed during a snow storm early in the season but did not persist, with open water observed until the first persistent ice set up on November 13, determined to be the date of freeze-up. Here, freeze-up was a result of a combination of advection of ice formed offshore and *in situ* freezing. For local ice use, the strength of the ice is particularly relevant, with a key criterion being sufficient thickness to walk on the ice.

Observations and analysis of freeze-up and break-up as described above were used in developing a statistical algorithm to be applied to the SSM/I and SSMI/S data to calculate freeze-up and break-up dates. The algorithm is described here and applied to the satellite record from October 28, 1978, through September 30, 2013. The algorithm was derived by comparing three different approaches to determine freeze-up and

break-up dates based on time series of satellite ice concentration obtained from passive microwave data (M.-L. Kapsch and H. Eicken, unpublished) and selecting the algorithm that showed the smallest deviations between ground-based observations and remote sensing data. We focus in this paper on the northeastern Chukchi Sea and southern Beaufort Sea coasts near Barrow, Alaska.

The SSMR, SSM/I and SSMI/S sea-ice concentration data derived using the NASA Team algorithm were extracted from several platform frequencies and polarizations (Cavalieri et al., 1996). The SMMR data span 1978 to 1987 and the follow-up SSM/I onboard Defense Meteorological Satellite Program (DMSP) satellites F8, F11, and F13 cover 1987 through 2007. Beginning in January 2007 SSMI/S data collected aboard DMSP-F17 have become available. The SMMR data were collected every other day with gaps in August 1982 and 1984. The SSM/I and SSMI/S data were collected daily with a data gap from December 3, 1987 to January 13, 1988. The NASA Team algorithm uses the multi-frequency brightness temperature data to calculate total ice concentration, mapped to a 25-km polar stereographic grid, from which total ice area and total ice extent are derived. These data, readily available through the National Snow and Ice Data Center, and based on GHz frequency microwave (millimeter to centimeter wavelengths) satellite radiance measurements, are among the best known, well validated, long-term, and pan-Arctic sea-ice records.

The sea-ice concentration grid points in this study (Figure 2) are located in the coastal Chukchi and Beaufort Seas. Grid points in proximity to land may be subject to errors from land-to-ocean spillover due to the coarseness of the satellite antennae pattern. Strong brightness temperature contrasts that are smeared across grid points can lead to falsely high estimates of sea-ice concentration. Spillover varies in time and is particularly important in late summer when there is open water near the coast.

To address this problem, the NASA Team algorithm applies the method detailed in Cavalieri et al. (1999) where "excess" concentration, the amount above a minimum threshold, is subtracted from concentration at coastal grid points. Monthly minimum concentration thresholds were established from 1984 and 1992 data. The spillover correction reduces values to the minimum threshold and was applied to daily sea-ice concentrations at grid points in the vicinity of land and open water. Figure 2 in Cavalieri et al. (1999) shows the 7 x 7 array defining the coastal grid point neighborhood, and their Figure 3 displays the results of applying the spillover correction. The correction scheme "reduces substantially the land spillover" (Cavalieri et al., 1999).

To evaluate the data used here for possible spillover, we visually inspected time series of summer sea-ice concentration in both the Chukchi and Beaufort regions. Ice concentration decreases in the offshore direction with grid points closest to shore generally having sea-ice concentrations that vary in time between 0% and ~ 20%. For this study we calculated the average ice concentration from August through September from a set of grid points to establish a summer concentration threshold used in freeze-up. The two-month average is expected to reduce any remaining spillover effects that are not constant in time.

NSIDC overview documents (nsidc.org) state that these data are within ± 15% of the actual summer concentration in the presence of summer melt ponds and within ± 5% of the actual winter concentration. In winter when the ice concentration is high, we expect the break-up computations to be robust. In the following discussions the decreasing accuracy of the data as the proportion of thin ice increases, and potential issues with summer data when melt is present or when there is significant new sea ice forming, must be kept in mind.

Different approaches to defining freeze-up and break-up using time series of ice concentration derived from passive microwave data were compared (M.-L. Kapsch and H. Eicken, unpublished). The definitions and algorithm used in this paper and summarized in Table 1 provide the closest approximation to freeze-up and break-up dates as defined by local observers for the local area of coastal ocean near the Alaska coastal communities of Gambell, Wales and Barrow (Eicken et al., 2014).

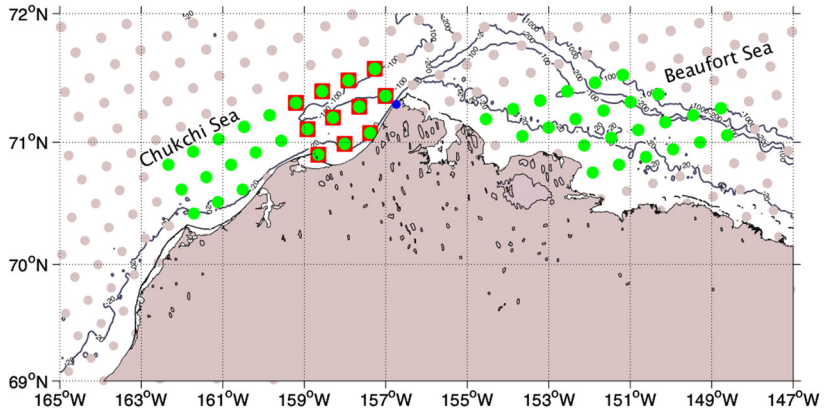

Figure 2

NSIDC grid points for the coastal Chukchi and Beaufort Seas.

The 25-km NISDC grid points are marked by light tan dots. Green dots in the west denote "Chukchi", in the east "Beaufort", and red squares mark the subset for "Barrow". The Chukchi and Beaufort sets are each 24 points. Barrow is marked by the blue dot.

doi: 10.12952/journal.elementa.000124.f002

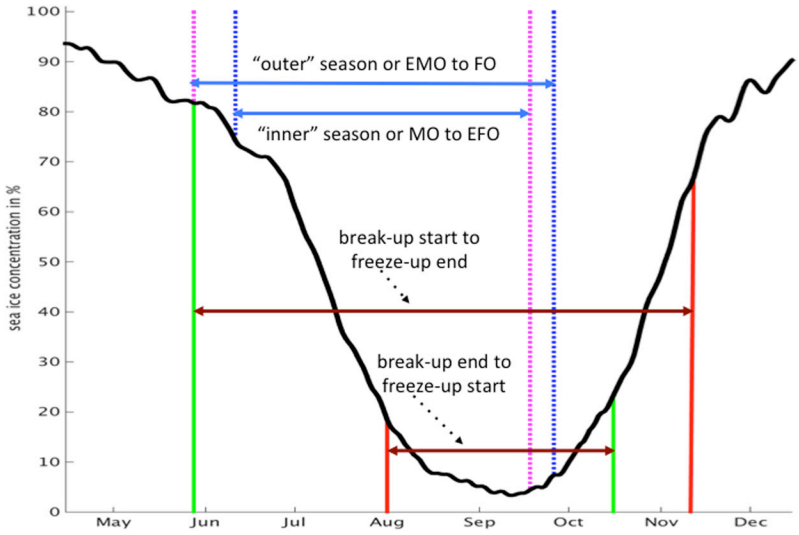

Figure 3

Seasonal timing and the climatological sea-ice cycle.

Climatology of the 1979–2007 sea-ice concentration for the combined Chukchi/Beaufort coastal region is shown by the solid black line from May through December. The computed start date for freeze-up and break-up are both marked by solid green lines. The end dates for freeze-up and break-up are marked by solid red lines. Seasonal durations are shown by dark red arrows from "break-up start to freeze-up end" and "break-up end to freeze-up start". Dates from Markus et al. (2009) for early melt onset and early freeze onset from their Chukchi/Beaufort Seas region are shown by the dotted magenta lines, and melt onset and freeze onset by dotted blue lines. Their "inner" and "outer" seasonal durations are marked by blue arrows.

doi: 10.12952/journal.elementa.000124.f003

Binary data were downloaded from the NSIDC website, linearly interpolated to daily values of sea-ice concentration centered on noon, and spatially averaged as described below. The time series data were Hanning smoothed (weights of 0.25 to 0.5 to 0.25) to reduce short-term events lasting less than ~ 3 days. This shifts some freeze-up and break-up dates toward climatological values.

For convenience we define the sea-ice year from September 1 to August 31 of the following year. Calculating freeze-up start from the criteria listed in Table 1 requires a summer average (August–September) sea-ice concentration. A threshold is set each year to the larger of the summer average sea-ice concentration plus one standard deviation of the August through September concentrations, or 15%. Once a threshold is set, it is compared with the concentrations from the daily time series beginning September 1. Freeze-up start is the date when the ice concentration first exceeds this threshold. To calculate freeze-up end, a threshold of the average winter (January–February) concentration minus 10% is set. Freeze-up end is the first date when the daily time series concentration exceeds the threshold.

To calculate break-up start, a threshold is set to the winter (January–February) average concentration minus two standard deviations of the January through February concentrations. Daily concentrations within a two-week window beginning January 1 are compared to the threshold value. If all daily concentrations exceed the threshold, the next day is evaluated. Break-up start is the last day in the two-week window when all values exceed the threshold. Break-up end sets a threshold to the average summer (August–September) concentration plus one standard deviation of the August through September concentrations, with a minimum threshold of 15%. Break-up end is the last day to exceed the threshold. Note that the algorithm requires the *summer* sea-ice concentration to calculate a break-up end date that generally occurs in the *spring*. When the August–September average sea-ice concentration exceeds 25%, the dates for freeze-up start and break-up end are not calculated. When the summer sea-ice concentration exceeds 40%, freeze-up end and break-up start dates are not calculated.

Daily time series of sea-ice concentration were created for the three sets of grid points shown in Figure 2 and are referred to in the following discussions as Chukchi, Beaufort, and Barrow. A daily climatology was computed for each set as the 34-year (1978 to 2013) mean at each Julian Day. Dates of freeze-up and break-up were calculated using the algorithm described above and in Table 1 from the daily data and from the climatology sea-ice concentration time series.

5. Results

The algorithm described here determines dates that capture sea-ice behavior important to indigenous experts and ice users who depend on detailed knowledge of the seasonal ice cycle. The algorithm uses thresholds that vary in time. Each year, the "summer" and "winter" ice conditions are used to determine when freeze-up and break-up occur, consistent with ice observers describing freeze-up and break-up as a relative annual measure. This approach is different from applying a fixed concentration threshold, such as 15%, to determine ice season length (Parkinson, 2014).

A schematic of freeze-up and break-up seasonality using this approach (Figure 3) shows the mean start and end dates of freeze-up and break-up calculated from the algorithm described above for the entire set of coastal grid points (Figure 2) for the period of 1979–2007. Also shown are the transition dates and

melt season lengths (the "inner" and "outer" seasons as described previously) for the same period in the "Chukchi/Beaufort seas" region examined by Markus et al. (2009). Their "Chukchi/Beaufort seas" region extends from Bering Strait to ~ 81°N and from Wrangel Island to Banks Island (see their Figure 8). The lengths of the two seasons from our study differ more than the two seasons from Markus et al. (2009). Our approach separates well the annual cycle and marks the start and end of rapid sea-ice transitions in fall and spring.

Calculated freeze-up and break-up dates and linear trends from this study and Markus et al. (2009) are listed in Table 2. Compared to Markus et al. (2009), freeze-up start is 26 days later than early freeze onset (October 16 compared to September 19), freeze-up end is 46 days after freeze onset, break-up start is the same as early melt onset, and break-up end is 51 days after melt onset. While the mean dates are different, as expected, the trends from this study and from Markus et al. are all identical in sign. The freezing season trends have similar magnitude while the melt season trends from this study are more than twice that found by Markus et al. (2009).

Table 2. Comparison of sea-ice cycle phenologies for the Chukchi/Beaufort Seas, 1979—2007

This study			Markus et al. (2009)		
Timing Feature	Mean date or duration[a]	Trend[b] (days per decade)	Mean date or duration[a]	Trend[b] (days per decade)	Timing feature[c]
Freeze-up start	Oct 16	10.3*	Sep 19	8.4**	EFO
Freeze-up end	Nov 12	9.9*	Sep 27	6.9**	FO
Break-up start	May 28	–7.8	May 28	–2.8*	EMO
Break-up end	Aug 1	–8.9	Jun 11	–3.5**	MO
Break-up end to freeze-up start	78 days (27)	17*	99.4 days (14.6)	12**	MO to EFO
Break-up start to freeze-up end	174 days (29)	13*	121 days (13.9)	9.7**	EMO to FO

[a]Standard deviation in parentheses. For this study, n = 24 (freeze-up) and n = 20 (break-up).
[b]Asterisk indicates significant trend at the 95% level; two asterisks, at the 99% level.
[c]EFO indicates early freeze onset; FO, continuous freeze onset; EMO, early melt onset; MO, continuous melt onset.
doi: 10.12952/journal.elementa.000124.t002

Freeze-up and break-up dates calculated on the 1979–2013 climatology for the Chukchi and Beaufort coastal regions are listed in Table 3. The freeze-up season is shorter and break-up season is longer in the Beaufort Sea than in the Chukchi Sea. Climatological freeze-up starts almost a week earlier and ends two weeks earlier in the Beaufort Sea than in the Chukchi Sea. The duration of freeze-up is shorter by about ten days for the Beaufort Sea. Climatological break-up begins about a week earlier and ends ten days later in the Beaufort Sea than the Chukchi Sea with the climatological break-up duration of about 90–100 days, similar for both regions.

Table 3. Climatological freeze-up and break-up dates with seasonal durations for the Chukchi and Beaufort Sea coastal regions, 1979–2013

Timing feature	Chukchi Sea	Beaufort Sea
Freeze-up start	October 9	October 3
Freeze-up end	December 1	November 14
Freeze-up duration	53 days	42 days
Break-up start	May 2	April 24
Break-up end	August 1	August 10
Break-up duration	91 days	108 days
Break-up end to freeze-up start	69 days	54 days
Break-up start to freeze-up end	213 days	204 days

doi: 10.12952/journal.elementa.000124.t003

Mean dates for freeze-up and break-up and trends from 1979 to 2013 are listed in Table 4. The mean freeze-up start date is 5 days earlier in the Beaufort Sea than in the Chukchi Sea, and freeze-up end is 10 days earlier in the Beaufort Sea than the Chukchi Sea. The duration of freeze-up is similar for both regions, about 20 days. Linear trends over the record length indicate a delay in freeze-up by one to two weeks per decade with the largest trend for freeze-up start in the Chukchi. Record-length mean dates of break-up start and end are similar for the Chukchi and Beaufort Seas, with break-up arriving earlier by 5 to 12 days per decade. The trends are significantly different from zero at the 95% level.

Table 4. Mean freeze-up and break-up dates and trends for the Chukchi and Beaufort Sea coastal regions, 1979–2013

Timing feature	Chukchi Sea			Beaufort Sea		
	Mean date or duration[a]	Trend (days per decade)[b]	r	Mean date or duration[a]	Trend (days per decade)[b]	r
Freeze-up start	October 21	14	0.6	October 16	7	0.6
Freeze-up end	November 10	11	0.3	October 30	9	0.4
Freeze-up duration	22 days	-5	–0.3	18 days	1	0.1
Break-up start	May 24	-9	–0.1	May 26	–5	–0.1
Break-up end	July 28	-12	–0.3	August 1	–10	–0.4
Break-up duration	58 days	-2	–0.1	68 days	–6	–0.2
Break-up end to freeze-up start	97 days (34)	22 (27)	0.6	79 days (25)	16 (25)	0.6
Break-up start to freeze-up end	174 days (38)	18 (33)	0.5	158 days (31)	14 (33)	0.5

[a]Standard deviation in parentheses.
[b]N values in parentheses.
doi: 10.12952/journal.elementa.000124.t004

Mean dates of freeze-up and break-up for the Barrow daily data and for climatology are shown in Figure 4 for two seasonal cycles, 1997–1998 and 2005–2006. These years were selected to illustrate freeze-up and break-up differences and the algorithm's sensitivity to variations in the ice concentration time series. Year 1997-1998 had highly variable daily ice concentration in winter fluctuating between 50 and 100%. In contrast, year 2005-2006 had persistent 100% ice concentration for periods up to a month. There is close agreement between the daily data and climatology freeze-up end dates for both 1997 and 2005, and similarly close dates for break-up end for 1998 and 2006. Freeze-up start from daily data is later than climatology for both 1997 and 2005. Break-up start is later than climatology for both 1998 and 2006.

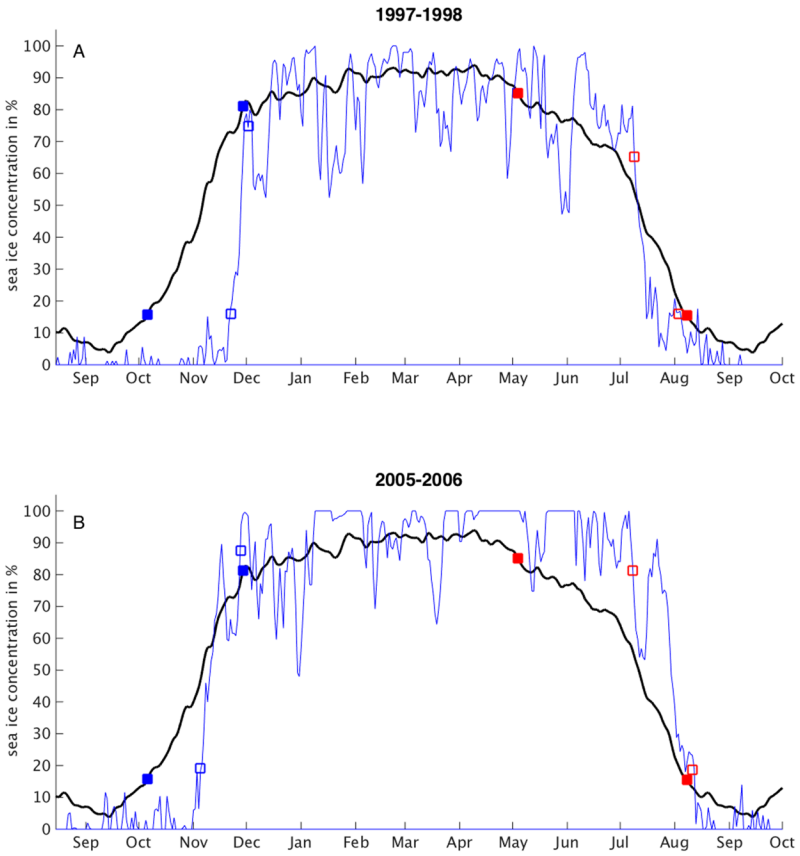

Figure 4

Sea-ice concentration record off Barrow, Alaska.

Calculated dates of freeze-up start and end (solid blue squares) and break-up start and end (solid red squares) are marked over the climatological (1978–2013) sea-ice concentration (thick black line) for Barrow. Calculated freeze-up and break-up dates are marked by open squares for the daily sea-ice concentration (thin blue line) for (A) 1997–1998 and (B) 2005–2006.

doi: 10.12952/journal.elementa.000124.f004

Figure 5 shows daily ice concentration for 1982 through 1986 over the (repeated) record-length climatology. September ice concentration exceeds climatology for summers of 1983 and 1985 that may be due to pack ice incursions that are well known to occur on the Chukchi coast. The most recent year for which local Iñupiaq ice experts reported such incursions was the summer of 2006, described by Richard Glenn from Barrow as similar to the types of ice conditions that were observed in the 1970s and 1980s, with ice lingering through summer into the freeze-up period (R. Glenn, personal communication, 2006).

When the summer ice concentration remains high, as shown in Figure 5, a calculation of break-up end is undefined in the current algorithm. This occurred in seven of the 35 years evaluated. In these years, ice remained along the coast for extended periods in summer. In some cases the ice concentration increased enough to significantly change the threshold but lasted for only a short period. Ice incursions and similar events described by local experts are detailed in Johnson et al. (2014).

The algorithm successfully calculates freeze-up and break-up start and end dates for every year after 1994. Figure 6 shows ice concentration for 2007 through 2012 when there were no summer ice incursions and the summer ice concentration fell to minimum levels each summer. The length of the summer ice-free season is clearly longer from 2007 onward than in 1983 and 1985 as shown in Figure 5.

The dates for freeze-up and break-up start and end for the Chukchi Sea region are plotted in Figure 7. There is substantial inter-annual variability with standard deviations of the mean dates at around three weeks. The correlation coefficient for freeze-up start is 0.6, freeze-up end is 0.4, break-up start is –0.4 and break-up end is –0.6. The linear fit shows freeze-up arriving later and break-up arriving sooner (values in Table 4). We identified outliers and years when freeze-up or break-up could not be calculated using the definitions from Table 1. These are listed in Table 5 to show that freeze-up or break-up could not be calculated for seven of the 34 record-length years, all of which are before 1995. Most of these years had significant summer ice present.

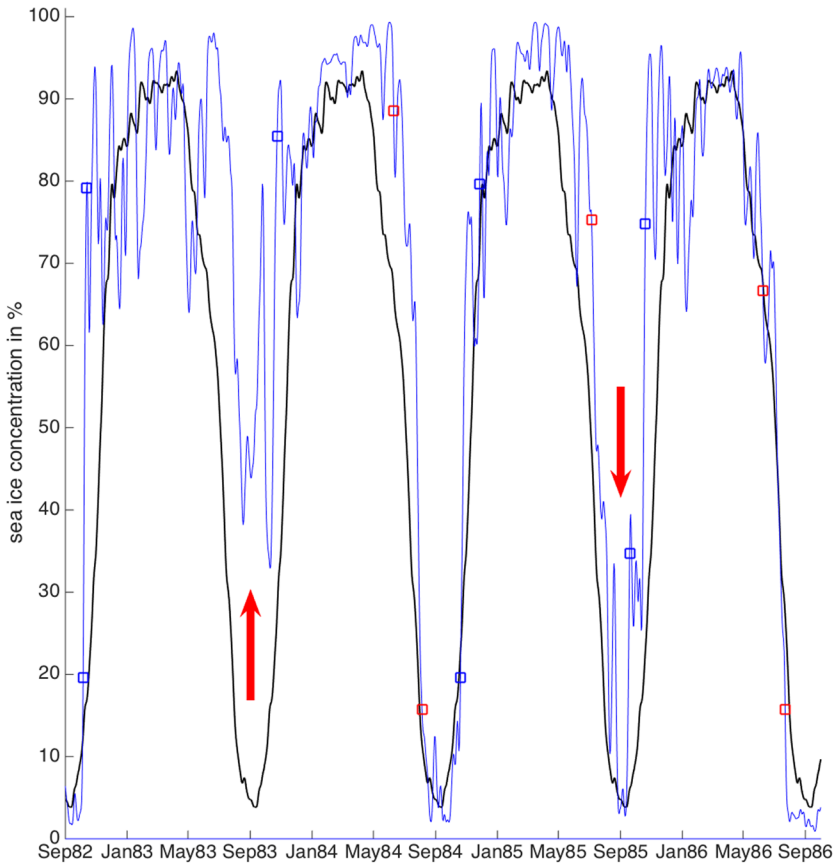

Figure 5

Freeze-up and break-up with two summer ice events.

Calculated dates of freeze-up (open blue squares) and break-up (open red squares) from 1982 through 1986 over daily sea-ice concentration (blue line) and the 34-year climatology (black line). Dates for end of break-up could not be calculated for 1983 and 1985 when significant ice (red arrows) remained in the region or was advected into the region during summer.

doi: 10.12952/journal.elementa.000124.f005

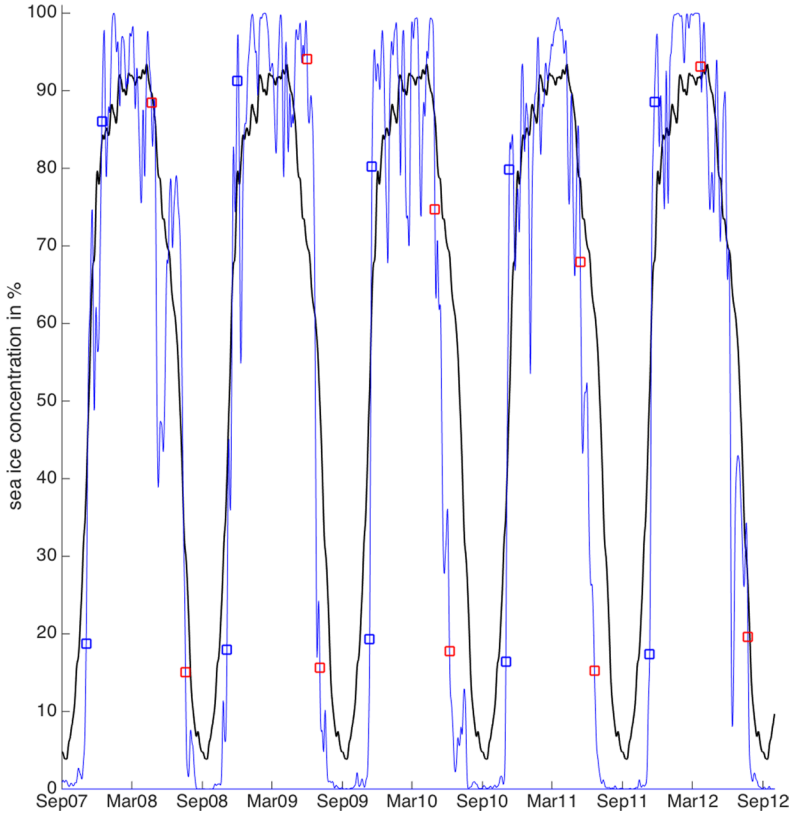

Figure 6

Freeze-up and break-up from 2007 to 2012.

Calculated dates of freeze-up (open blue squares) and break-up (open red squares) over daily sea-ice concentration (blue line) and the repeated 34-year climatology (black line). During summer in these years the sea-ice concentration is well below climatology and near zero. Extended winter periods of 100% ice concentration are absent.

doi: 10.12952/journal.elementa.000124.f006

Table 5. Freeze-up and break-up outlier dates[a]

Year	Break-up				Freeze-up				Comments
	Start		End		Start		End		
	Early	Late	Early	Late	Early	Late	Early	Late	
1980			NC						early summer ice, stays above 10% all summer
1981			NC						early summer peak in ice
1983	NC		NC		NC				summer ice above 30%
1985			NC						ice stays late into summer
1988			NC		NC				ice stays late into summer
1989							x		little summer ice
1990						x			late but rapid freeze-up
1991				x	x				break-up stalls at 40%
1992		x	NC		x				freeze-up start shows early ice peak of 45%
1993	x					x			long, ice free summer
1994		x	NC		x		x		rapid, steep freeze-up
1995				x			x		break-up stalls at 70%. early freeze-up to 85%
1996		x							late break-up start detected
1997						x			late freeze-up, steep, short
1998		x				x		x	break-up has false start
2001		x		x					break-up has two peaks between start and end
2004								x	freeze-up stalls
2010			x						break-up appears early

[a]NC indicates date could not be calculated; x indicates feature described in comments column.

doi: 10.12952/journal.elementa.000124.t005

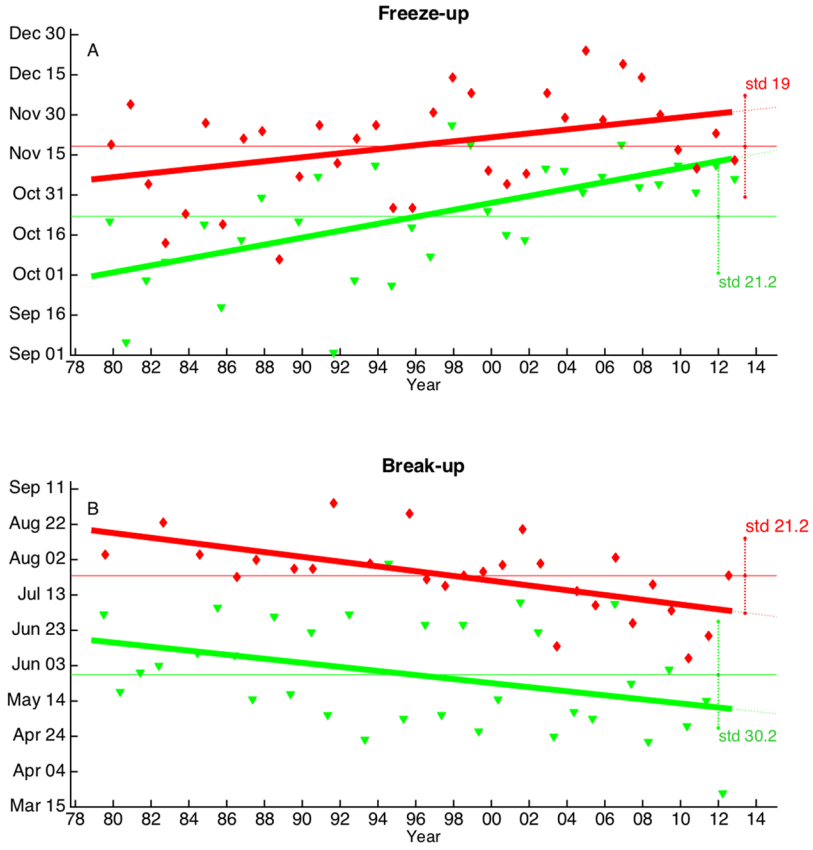

Figure 7

Chukchi Sea break-up and freeze-up dates.

Chukchi Sea (A) freeze-up start (green) and end (red) dates and (B) break-up start (green) and end (red) dates with linear trends. Freeze-up start delays by 14 days per decade and freeze-up end delays by 11 days per decade. The mean duration of freeze-up is 22 days. Break-up start begins earlier by 9 days per decade and break-up end begins earlier by 12 days per decade. The mean duration of break-up is 58 days. The x-axis is from 1978 to 2014. The y-axis limits are dates of the month. The standard deviations of the mean dates (horizontal lines) are shown at right (dotted vertical lines).

doi: 10.12952/journal.elementa.000124.f007

6. Discussion

The algorithm that was applied to ice concentration time series arose following discussions with indigenous sea-ice experts who regularly observe and use sea ice. Based on those discussions, we constructed an algorithm to define the seasonal ice cycle by calculating dates of freeze-up and break-up start and end. A comparison between freeze-up start and end dates to local observations (Figure 8) provides an indication of the uncertainty associated with the passive microwave data as to the onset and termination of freeze-up. This uncertainty is reflected for specific years in anomalies associated with a substantial discrepancy between passive microwave data and local observations or between local observations and webcam/photo records.

Most observations straddle the identity line where observations and the calculated dates agree, but data for 2006 and 2007 deviate significantly. For 2006, this deviation is explained by the delay in the formation of persistent, stable coastal and shorefast ice during a year with freeze-up dominated by advection into and export out of the area along with late local ice formation. As reported by J. M. Leavitt and A. Brower, Sr., ice kept forming and melting or being advected offshore with open water persisting over large areas from the beach outward through mid-December. On December 15 the first persistent young ice took hold alongshore; this ice was deemed safe to walk on the following day, but with large areas of open water remaining (Leavitt, in Apangalook et al., 2013). In 2007, a different mode of freeze-up occurred at Barrow, with young ice forming and persisting nearshore from November onwards. As confirmed by local experts, such ice can form in shallows or lagoons and persist alongshore despite the absence of extensive pack ice offshore.

The uncertainties evident in Figure 8 in defining a single freeze-up date reflect the recognition by local experts and other ice users (such as the maritime industry) that with a combination of *in situ* ice formation and advective processes at a particular location, freeze-up is an extended period whose bounds depend on the specific ice use or definition of freeze-up. The same holds for break-up in the spring. The definitions for both events in the seasonal cycle, and their start and end dates, reflect this fact and may hence be of value from an operational or ice use perspective.

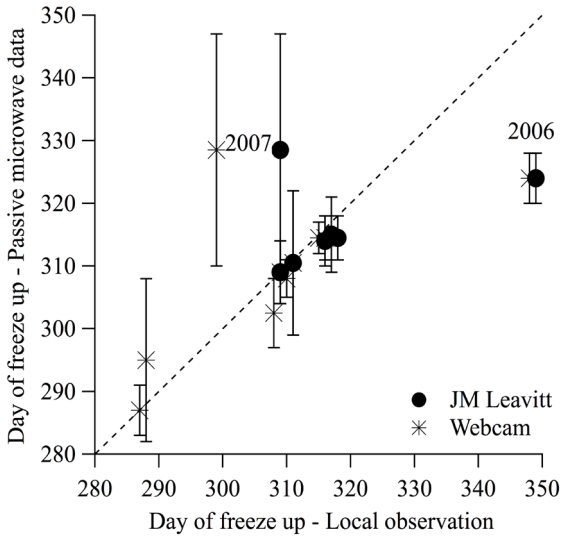

Figure 8

Comparison of freeze-up start and end dates.

Comparison of freeze-up period derived from passive microwave satellite data with that derived from local observations at Barrow by observer Joe M. Leavitt and from webcam/photographic images. Symbols mark mid-point of freeze-up interval, vertical lines indicate range from start to end of freeze-up. The 2006 and 2007 outliers are discussed in the text. The dotted line marks the one-to-fit where local observations equal day of freeze-up from passive microwave data.

doi: 10.12952/journal.elementa.000124.f008

From 34 years of satellite data the calculated trends of delayed freezing and earlier melting are consistent in sign and general magnitude with those of Markus et al. (2009), Mortin et al. (2014), and Brown et al. (2014). We can use the calculated long-term trends in the Chukchi Sea to extrapolate freeze-up and break-up dates for a future year. While the choice of a future year is somewhat arbitrary, we first choose 2030 as an example, in part because Overland and Wang (2013) label 2030 as a midpoint among time horizons for a "nearly sea-ice free summer" Arctic. The linear projection from data presented here is for freeze-up to start on December 6 and end on December 13, 2030. Break-up start projects to April 19 and break-up end projects to June 10. These results indicate that by around 2030, the open water season between break-up end and freeze-up start, is from early June until early December, a range nearly twice the 1978-2013 mean range of 97 days (see Table 4).

With freeze-up arriving later and break-up earlier, we can also determine from the trends the year when they coincide. At such a time we assume there would be no "winter" season because the ice would break-up as soon as it freezes-up. From this study's linear projections, freeze-up ends and break-up begins around the same time in 2100. In February–March 2100, there is no duration for the frozen season such that a "solid" winter ice cover might not form. While the trends are clear, this analysis is a local one focusing on the Chukchi and Beaufort coasts. We know of no reason to support the assumption that a linear trend would be sustained even as the ice cover undergoes major change. Rather, non-linear adjustments are likely, hence the need for long-term tracking of ice conditions.

The trends of later freezing and earlier melting raise questions about the role of sea-ice advection into the Chukchi Sea because advection of ice into a region affects the calculation of the date of break-up. There are seven years where break-up could not be calculated (Table 5), and they all fall before 1995, consistent with a possible retreat of the ice pack. We noted above the possible interpretation that by 2100 the sea ice may retreat poleward of Barrow. To examine this possibility, we analyzed where the 15% sea-ice concentration (also used by Mortin et al., 2014 to help constrain melt-freeze transition dates) fell on longitude 169°W (longitude of Bering Strait) from 1979 through 2013. The 15% isoline was found to retreat poleward at this longitude at a rate of ~ 250 km per decade. If this trend persists, then the 15% isoline retreats to the pole by 2100. In this case, sea-ice incursions from the central Arctic pack may be the dominant source of summer season ice in the Chukchi Sea.

Inspection of the break-up start dates (Figure 7B) shows eleven years well below the regression line. To focus on these "early" break-up years, a Hovmöller diagram was constructed of sea-ice concentration anomalies (annual cycle removed) for the Chukchi points shown in Figure 2. This diagram (Figure 9) shows an oscillation in break-up start (green line) that is strongly bi-annual from 1982 through 2000 where early break-up years alternate with later break-up years that are generally later by about a month. Selecting only the "early break-up start" dates gives a linear correlation coefficient of -0.88, indicating a strong, linear trend for earlier "early" break-up start (black trend line in Figure 9). Since 1979, early break-up has become earlier by more than one month.

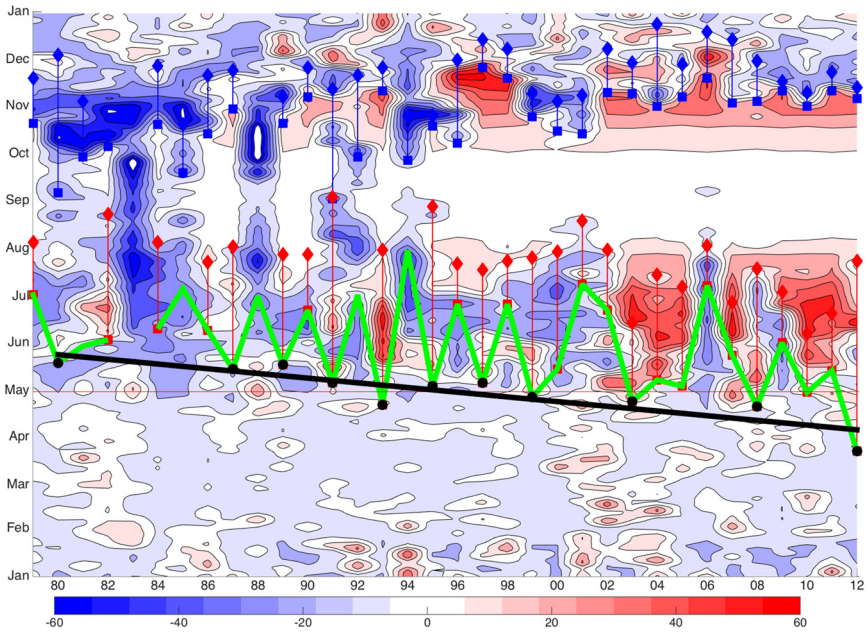

Figure 9

Sea-ice concentration anomaly from 1979 through 2012.

Sea-ice concentration anomaly (color scale bar) with the annual cycle removed contoured as a Hovmöller diagram from 1979 through 2012 (x-axis). The green line connects dates of break-up start and suggests a quasi bi-annual oscillation. The linear fit (black line connecting black circles) to "early" break-up start dates (see text) has a correlation coefficient of −88. Red symbols mark the beginning and end of break-up. Blue symbols mark the beginning and end of freeze-up. Durations of freeze-up and break-up are marked by the vertical lines.

doi: 10.12952/journal.elementa.000124.f009

7. Summary

Based on discussions with sea-ice experts having experience observing and working on the sea ice in the Bering, Chukchi and Beaufort Seas, a statistical algorithm was developed and applied to time series of satellite-derived sea-ice concentration from 1979 to 2013. The method described in this paper provides an internally consistent and reproducible approach to characterize the annual sea-ice cycle by calculating dates of start and end of freeze-up and break-up.

The long-term trends in freeze-up reveal delays in the freeze-up season of about two weeks per decade for the Chukchi and one week per decade for the Beaufort coastal regions. Break-up start is arriving sooner by about a week per decade and break-up end is arriving earlier by 10 to 12 days per decade. There is evidence of a quasi bi-annual oscillation in break-up start and a trend for early break-up start arriving sooner by more than one month over the 34-year record length.

The sea-ice phenology of freeze-up and break-up that emerges is consistent with observations of sea ice in terms of sea-ice use (e.g., subsistence hunting), navigation, and as an ecological platform. Dates of freeze-up and break-up might be used to anticipate the open water season and navigation windows, or to help quantify discussions of habitat availability for organisms using the ice for reproduction and/or feeding. Additionally, we expect to use the algorithm on ice concentration time series from numerical model results to determine model timing of the sea-ice cycle and compare it to the timing extracted from the satellite record.

The algorithm described here provides an approach to calculating dates of sea-ice freeze-up and break-up based upon the statistical behavior of sea-ice concentration from the satellite record. Freeze-up and break-up dates may be used to provide information helpful to understanding the dynamics of the annual sea-ice cycle and further identifying the drivers that modify this cycle.

References

Anderson M. 1987. The onset of spring melt in first-year ice regions of the Arctic as determined from Scanning Multichannel Microwave Radiometer data for 1979 and 1980. *J Geophys Res* **92**(C12): 13153–13163. doi: 10.1029/JC092iC12p13153.

Apangalook L, Apangalook P, John S, Leavitt J, Weyapuk W Jr, et al. 2013. Local Observations from the Seasonal Ice Zone Observing Network (SIZONet). *[Observations by Leavitt JM and Brower A, Sr]*. Boulder, Colorado USA: National Snow and Ice Data Center. http://dx.doi.org/10.7265/N5TB14VT. Eicken H, Kaufman M, eds.

Baordo F, Geer A. 2015. Microwave surface emissivity over sea-ice. *EUMETSAT Satellite application facility on numerical weather prediction (NWP SAF)*. https://nwpsaf.eu/publications/vs_reports/nwpsaf-ec-vs-026.pdf. Accessed June 2015.

Barnhart KR, Anderson RS, Overeem I, Wobus C, Clow GD, et al. 2014. Modeling erosion of ice-rich permafrost bluffs along the Alaskan Beaufort Sea coast. *J Geophys Res: Earth Surf* **119**: 1155–1179. doi: 10.1002/2013JF002845.

Barry RG, Moritz RE, Rogers JC. 1979. The fast ice regimes of the Beaufort and Chukchi Sea Coasts, Alaska. *Cold Reg Sci Technol* **1**(2): 129–152. doi: 10.1016/0165-232X(79)90006-5.

Bitz CM, Battisti DS, Moritz RE, Beesley JA. 1996. Low-frequency variability in the Arctic atmosphere, sea ice, and upper-ocean climate system. *J Clim* **9**: 394–408. doi: 10.1175/1520-0442(1996)009<0394:LFVIT>2.0.CO;2.

Bitz CM, Roe GH. 2004. A mechanism for the high rate of sea ice thinning in the Arctic Ocean. *J Clim* **17**: 2623–2632. doi: 10.1175/1520-0442(2004)017<3623:AMFTHR>2.0.CO;2.

Bjørgo E, Johannessen O, Miles M. 1997. Analysis of merged SMMR-SSMI time series of Arctic and Antarctic sea ice parameters 1978–1995. *Geophys Res Lett* **24**(4): 413–416. doi: 10.1029/96GL04021.

Brown L, Howell S, Mortin J, Derksen C. 2014. Evaluation of the interactive multisensor snow and ice mapping system (IMS) for monitoring sea ice phenology. *Remote Sens Environ* **147**: 65–78. doi:10.1016/j.rse.2014.02.012

Cavalieri DJ, Parkinson CL, Gloersen P, Comiso JC, Zwally HJ. 1999. Deriving long-term time series of sea-ice cover from satellite passive-microwave multisensor data sets. *J Geophys Res* **104**(C7): 15803–15814. doi: 10.1029/1999JC900081.

Cavalieri DJ, Parkinson CL, Gloersen P, Zwally H. 1996. Sea ice concentrations from Nimbus-7 SMMR and DMSP SSM/I-SSMIS passive microwave data, Version 1. (Updated yearly). *NASA National Snow and Ice Data Center Distributed Active Archive*. Boulder, Colorado USA. http://dx.doi.org/10.5067/8GQ8LZQVL0VL. Accessed March 2014.

Comiso JC. 2002. A rapidly declining perennial sea ice cover in the Arctic. *Geophys Res Lett* **29**(20): 1956. doi:10.1029/2002GL015650.

Drobot SD, Anderson MR. 2001. An improved method for determining snowmelt onset dates over Arctic sea ice using scanning multichannel microwave radiometer and Special Sensor Microwave/Imager data. *J Geophys Res* **106**(D20): 24033–24049. doi:10.1029/2000JD000171.

Eicken H. 2013. Ocean science: Arctic sea ice needs better forecasts. *Nature* ***497***(7450): 431–433. doi: 10.1038/497431a.

Eicken H, Gradinger R, Salganek M, Shirasawa K, Perovich DK, et al., eds. 2009. *Field Research Techniques for Sea Ice Research*. Fairbanks, Alaska: University of Alaska Press.

Eicken H, Kaufman M, Krupnik I, Pulsifer P, Apangalook L, et al. 2014. A framework and database for community sea ice observations in a changing Arctic: An Alaskan prototype for multiple users. *Polar Geogr* **37**(1): 5–27. doi: 10.1080/1088937X.2013.873090.

Eicken H, Mahoney AR. 2015. Sea ice: Hazards, risks and implications for disasters, in Ellis J, Sherman D, eds., *Sea and Ocean Hazards, Risks and Disasters*. Oxford: Elsevier: pp. 381–401.

Holland MM, Bitz CM, Tremblay B. 2006. Future abrupt reductions in the summer Arctic sea ice. *Geophys Res Lett* **33**: L23503. doi: 10.1029/2006GL028024.

Johnson MA, Eicken H, Druckenmiller ML, Glenn R, eds. 2014. Experts workshops to comparatively evaluate coastal currents and ice movement in the northeastern Chukchi Sea; Barrow and Wainwright, Alaska, March 11–15, 2013. Fairbanks, Alaska: University of Alaska Fairbanks. https://www.uaf.edu/sfos/research/projects/experts-workshops-to-comp/publications-products/index.xml. Accessed June 2015.

Kovacs A, Mellor M. 1974. Sea ice morphology and ice as a geologic agent in the southern Beaufort Sea, in Reed JC, Sater JE, eds., *The Coast and Shelf of the Beaufort Sea*. Arlington VA: The Arctic Institute of North America.

Laidler GJ, Ford JD, Gough WA, Ikummaq T, Gagnon SA, et al. 2009. Travelling and hunting in a changing Arctic: Assessing Inuit vulnerability to sea ice change in Igloolik, Nunavut. *Climatic Change* **94**(3–4): 363–397. doi: 10.1007/s10584-008-9512-z.

Lovecraft AL, Meek CL, Eicken H. 2013. Connecting scientific observations to stakeholder needs in sea ice social-environmental systems: The institutional geography of northern Alaska. *Polar Geogr* **36**: 105–125. doi: 10.1080/1088937X.2012.733893.

Mahoney AR, Eicken H, Gaylord AG, Gens R. 2014. Landfast sea ice extent in the Chukchi and Beaufort Seas: The annual cycle and decadal variability. *Cold Reg Sci Technol* **103**: 41–56. doi: 10.1016/j.coldregions.2014.03.0033.

Markus T, Stroeve J, Miller J. 2009. Recent changes in Arctic sea ice melt onset, freezeup, and melt season length. *J Geophys Res* **114**: C12024. doi: 10.1029/2009JC005436.

Mortin J, Howell S, Wang L, Derksen C, Svensson G, et al. 2014. Extending the QuikSCAT record of seasonal melt-freeze transitions over Arctic sea ice using ASCAT. *Remote Sens Environ* **141**: 214–230. doi: 10.1016/j.rse.2013.11.004.

NSIDC - National Snow and Ice Data Center. 2013. Sea Ice Concentrations from Nimbus-7 SMMR and DMSP SSM/I-SSMIS Passive Microwave Data, Version 1. http://nsidc.org/data/docs/daac/nsidc0051_gsfc_seaice.gd.html Accessed November 2015.

Overland J, Wang M. 2013. When will the summer Arctic be nearly sea ice free? *Geophys Res Lett* **40**: 2097–2101. doi: 10.1002/grl.50316.

Parkinson CL. 2014. Spatially mapped reductions in the length of the Arctic sea ice season. *Geophys Res Lett* **41**(12): 4316–4322. doi: 10.1002/2014GL060434.

Parkinson CL, Cavalieri D, Gloersen P, Zwally H, Comiso J. 1999. Arctic sea ice extents, areas, and trends, 1978–1996. *J Geophys Res* **104**(C9): 20837–20856. doi: 10.1029/1999JC900082.

Perovich D, Jones KF, Light B, Eicken H, Markus T, et al. 2011. Solar partitioning in a changing Arctic sea-ice cover. *Ann Glaciol* **52**(57): 192–196. doi: 10.3189/172756411795931543.

Perovich D, Nghiem SV, Markus T, Schweiger A. 2007. Seasonal evolution and interannual variability of the local solar energy absorbed by the Arctic sea ice-ocean system. *J Geophys Res* **112**: C03005. doi: 10.1029/2006JC003558.

Perovich D, Polashenski C. 2012. Albedo evolution of seasonal Arctic sea ice. *J Geophys Res* **39**(8): L08501. doi: 10.1029/2012GL051432.

Petrich C, Eicken H, Polashenski CM, Sturm M, Harbeck JP, et al. 2012. Snow dunes: A controlling factor of melt pond distribution on Arctic sea ice. *J Geophys Res* **117**: C09029. doi: 10.1029/2012JC008192.

Post E, Bhatt US, Bitz CM, Brodie JF, Fulton TL, et al. 2013. Ecological consequences of sea-ice decline. *Science* **341**(6145): 519–524. doi: 10.1126/science.1235225.

Reimnitz E, Toimil L, Barnes P. 1978. Arctic continental shelf morphology related to sea-ice zonation, Beaufort Sea, Alaska. *Mar Geol* **28**: 179–210. doi: 10.1016/0025-3227(78)90018-X.

Rothrock D, Yu Y, Maykut G. 1999. Thinning of the Arctic sea-ice cover. *Geophys Res Lett* **26**: 3469–3472. doi: 10.1029/1999GL010863.

Serreze MC, Holland MH, Stroeve J. 2007. Perspectives on the Arctic's shrinking ice cover. *Science* **315**(5818): 1533–1536. doi: 10.1126/science.1139426.

Smith S, Muench R, Pease C. 1990. Polynyas and leads: An overview of physical processes and environment. *J Geophys Res* **95**(C6): 9461–9479. doi: 10.1029/JC095iC06p09461.

Stephenson SR, Smith LC, Agnew JA. 2011. Divergent long-term trajectories of human access to the Arctic. *Nat Clim Change* **1**(3): 156–160. doi: 10.1038/nclimate1120.

Stroeve J, Hamilton LC, Bitz CM, Blanchard-Wrigglesworth E. 2014a. Predicting September sea ice: Ensemble skill of the SEARCH Sea Ice Outlook 2008–2013. *Geophys Res Lett* **41**: 2411–2418. doi: 10.1002/2014GL059388.

Stroeve J, Markus T, Boisvert L, Miller J, Barrett A. 2014b. Changes in Arctic melt season and implications for sea ice loss. *Geophys Res Lett* **41**: 1216–1225. doi: 10.1002/2013GL058951.

Wadhams P, Davis NR. 2000. Further evidence of ice thinning in the Arctic Ocean. *Geophys Res Lett* **27**(24): 3973–3975. doi: 10.1029/2000GL011802.

Contributions

- Main concept and key ideas: MJ, HE
- Collection and compilation of observational data: HE
- Analysis and interpretation of data: MJ, HE
- Drafting of article and contribution of intellectual content: MJ, HE
- Final approval of the version to be published: MJ, HE

Acknowledgments

We acknowledge the important ground-based observations by Iñupiaq ice experts that helped guide this study. John "Craig" George also shared observations of freeze-up at Barrow. Marie-Louise Kapsch's help in early stages of this work is gratefully acknowledged. Comments by two anonymous reviewers helped improve the manuscript.

Funding information

Funding support of the Seasonal Ice Zone Observing Network (SIZONet) by the National Science Foundation helped generate some of the data underlying this work and is gratefully acknowledged.

Competing interests

The authors declare no competing interests.

Data accessibility statement

Sea ice concentration from October 1978 to December 2015 is available publically through the National Snow and Ice Data Center. doi: http://dx.doi.org/10.5067/8GQ8LZQVL0VL